©Freund Publishing House Ltd. International Journal of Turbo and Jet Engines, 25, 163-178 (2008)

Effects of Geometric and Structural Parameters ou Coupled Bending Torsion Flutter in Turbo Machinery Blades

H. Pathak, A. Kushari*, C. Venkatesan

Department of Aerospace Engineering, Indian Institute of Technology, Kanpur-208016, INDIA

Abstract

The development of propulsion system technology over the last few decades has encountered and overcome several technological barriers. A large number of problems were resolved resulting in considerably higher component efficiencies and reduced fuel consumption. These advances led to lighter overall designs and higher power densities compared to earlier designs. The accomplishment of lighter designs for the turbomachinery components also led to some drawbacks due to the reduced margins on the design factor-of-safety. Consequently, aeroelastic stability has become a major concern, and is often the limiting design constraint. So a careful and systematic study of coupled bending-torsion flutter of a cascade in incompressible flow was carried out which requires estimation of unsteady aerodynamic loads, and a structural model of the cascade. Unsteady aerodynamic loads were evaluated using Whitehead's solution for incompressible flow through a cascade of arbitrary geometry and interblade phase angle. The lift and moment coefficients calculated were found to match within the four decimal place accuracy with the results given by Whitehead and other literature. The blades were modeled as an equivalent 2-D section at 75% of span, and structural and inertial couplings were lumped into an effective CG-EA offset. Structural damping was included in the equations of motion. The resulting complex eigenvalue problem was solved recognizing the fact that there are two parameters in the eigenvalue problem, namely the reduced frequency k and the interblade phase angle β. The critical flutter speed was determined by minimizing it with respect to β, keeping the constraint on β as suggested by Lane. The solution provided the critical flutter speed with respect to both the torsion and the bending modes as a function of the interblade phase angle as well as dominant vibration frequencies at flutter. Various structural and aerodynamic parameters of the cascade were varied and the effect of the variations on the coupled bending torsion flutter was studied. A jump was observed in the flutter boundary near frequency ratio of 1, which was explained by the change in the mode shape of the vibration, which is represented by interblade phase angle. The developed technique can be used as a preliminary design tool for the aeroelastic flutter analysis of turbo-machinery blades.

Nomenclature

a	nondimensional location of elastic axis
a_c	$c/s \cdot \cos\xi$
[A]	aerodynamic matrix
b	semi-chord
b_c	$c/s \cdot \sin\xi$
c	2b = chord
C_{Fq}, $C_{Fα}$, C_{Fw}	nondimensional force coefficients
C_{Mq}, $C_{Mα}$, C_{Mw}	nondimensional moment coefficients
[C]	matrix of force and moment coefficients
G, H, I, J	coefficients in Series
h	bending deflection, positive down
k	ωb/U = reduced frequency
k', l, m	integers
n	integer giving order of approximation used
[K]	stiffness matrix
$[\bar{K}_d]$	nondimensionalized stiffness matrix with inclusion of structural damping
[M]	mass matrix
N_b	number of Blades
p	static pressure
P_E	exponent in complex eigenvalue problem
$qe^{\omega t}$	translational velocity of blades due to vibration

* Corresponding Author: Ph: 91-512-2597126, Fax: 91-512-2597626, Email: akushari@iitk.ac.in

r	integer
r_α	nondimensional radius of gyration
x_l	nondimensional CG-EA offset
s	cascade spacing
t	time
U	mainstream velocity
$ve^{i\omega t}$	velocity induced by vorticity on blades and their wakes
$we^{i\omega t}$	velocity of disturbances due to wakes from upstream obstructions
x, y	rectangular coordinates
$\alpha e^{i\omega t}$	torsional displacement of blades (positive anticlockwise)
β	interblade phase angle
γ	bound vorticity per unit length
γ_ω	ω_B/ω_T = Frequency Ratio
ε	shed vorticity
η	coordinate for induced velocity
θ	variable defined by $x = \frac{1}{2}(1-\cos\theta)$
λ	2k – Frequency parameter = $\omega c/U$
μ	mass ratio of blade = $m/\pi\rho b^2$
ξ	stagger angle of cascade
ρ	air density
ϕ	variable defined by $\eta = \frac{1}{2}(1-\cos\phi)$
ω	angular frequency of vibration

Introduction

In the operation of aircraft engines, the aeroelastic behavior of blades in fans and compressor could induce not only high cycle fatigue but also structural failure of the blades and, possibly, extensive damage to the engine with catastrophic consequences to the aircraft for which these engines provide the necessary thrust. The vibration leading to such failures can be stable, as in the case of forced vibrations from inlet distortion or blade row interactions, or they can be unstable, as in the case of self-exited vibrations or flutter. Because of the close interaction between performance and structural integrity, designers of aircraft engines must place great importance on aeroelastic effects to optimize a given design.

Blade flutter is observed when the vibration of the blades triggered by any temporary perturbation does not die away but is rather sustained through the energy fed into the structure by the unsteady aerodynamic forces caused by the vibration itself. Due to aerodynamic nonlinearities such as the unsteady motion of strong shocks or structural nonlinearities such as the mechanical damping of frictional contacts, this process may end up in a limit cycle. The High Cycle Fatigue (HCF) caused by these vibrations may shorten the life of the blades below the target life of the engine. The occurrence of flutter is due to the fact that the aerodynamic damping associated with certain flow regimes becomes negative and is not counterbalanced by the mechanical damping of the assembly. The key feature of the flutter is that the aerodynamic forces acting on the blades originate from the vibration of the blades themselves.

A basic introduction to the aeroelasticity of turbomachinery was given by Fleeter /1/. Various aeroelastic phenomena like flutter, forced response for compressor and fan were discussed. Earlier research on the turbomachinery aeroelasticity has concentrated on looking at the effect of the structural parameters on the stability boundaries, and the effect of aerodynamic parameters of a cascade, e.g., spacing to chord ratio, stagger angle, etc, were always ignored. Much of the earlier work in this area was experimental, partly due to the unavailability of a good unsteady aerodynamic model, and partly because of the mathematical difficulties and computational effort required to develop and implement a theory even for the simplest cases. Aeroelastic analysis of turbomachinery was done by Srivastava *et al.* /2,3/ using CFD (phase lagged boundary condition method). The results obtained were found to match with the experimental results available for fan configuration; however for the turbine configuration the results showed good trend wise behavior but differed in numerical values with the experimental results.

The case of a zero stagger cascade in which the blades vibrate out-of-phase with each other was

studied by Reissner /4/ and Lilley /5/. This is the simplest case to treat, since, by symmetry, the streamlines half-way between the blades are stationary with respect to time and may, therefore, be replaced by solid walls. This problem corresponds, therefore, to the case of a single airfoil vibrating in a wind tunnel, and was studied primarily for this reason. For a zero stagger angle and in phase vibration of all the blades, the problem was studied by Mendelson and Carrol /6/ and by Chang and Chu /7/.

An experimental flutter study with the aim to assess effects of blade mode shape on the aeroelastic stability of a typical aero engine low-pressure turbine blade row was done by Vogt and Fransson /8/. One blade in the cascade was made to oscillate and the pressure response data was acquired on the neighboring four blades.

The first attempt to get a generalized unsteady cascade theory was made by Sisto /9,10/. He obtained a solution for the case of an unstaggered cascade in incompressible flow vibrating with arbitrary phase angle. A more generalized study where both phase angle and stagger angle were arbitrarily changed was done by Lane and Wang /11/ and results for a cascade with 45 degree stagger were presented.

The first complete treatment of unsteady compressible flow through a cascade of arbitrary stagger and interblade phase angle was developed by Lane and Friedman /12/. They considered superposition of elementary solutions of the reduced wave equations, thus obtaining a dual set of integral equations for the Fourier transform of the pressure loading on the reference blade. These equations were solved by collocation. The results are in good agreement with calculations by Runyan, Woolston, and Rainey /13/ for the equivalent wind tunnel wall interference problem.

Whitehead /14/ later published a theory for incompressible flow and gave extensive numerical tables of forces and moment coefficients for a range of cascade parameters. His work was an extension of the work done by Theoderson /15/, who estimated the unsteady aerodynamic behavior of a single blade. Whitehead's basic approach was to replace the blades and their wakes by straight vortex sheets, and determine the distribution of bound vorticity which induces the correct upwash velocity along the blade chord. The resulting integral equation is solved by collocation to get the aerodynamic coefficients. Whitehead only considered SDOF (single degree of freedom) flutter and concludes that, under the assumption of the theory, bending flutter appears impossible. Torsional flutter, on the other hand, was found to occur over a range of cascade parameters, and was studied in detail in a later paper /16/. He concluded that torsional flutter is very sensitive to the location of the elastic axis, the best location being around ¼ chord and the worst location around ¾ chords. The theory was extended by Whitehead /17/ to include finite mean angle of attack, in an attempt to explain bending flutter.

The problem of coupled bending-torsion flutter in cascade was solved by Bendiksen and Friedmann /18/ with much emphasis on the effect of various structural parameters variation on the coupled bending-torsion flutter speed. The location of elastic axis and the distance between the elastic axis and center of mass were changed and the corresponding effect on flutter speed was studied. Also a comparison between the coupled bending-torsion flutter speed and the single degree of freedom flutter speed was made.

An investigation on the effects of mistuning on flutter and forced response of a cascade in subsonic and supersonic flows was done by Kielb and Kaza /19/. The aerodynamic and structural coupling between the bending and torsional motions and the aerodynamic coupling between the blades were included. It was shown that frequency mistuning always has a beneficial effect on flutter. Additionally, the results indicated that frequency mistuning may have either a beneficial or an adverse effect on forced response, depending on the engine order of the excitation and Mach number.

The aim of the present study is to analyze the effects of different structural and geometric

parameters on the coupled bending torsion flutter boundary and to study the effect of interblade phase angle on the flutter boundary. In earlier studies no attempt was made to explain the sudden jump in the flutter boundary near the frequency ratio value of one. The reason for this jump is also explained in the present study. The effects of space to chord ratio and stagger angle on the flutter boundary were also examined.

Theoretical Model of Cascade Flutter

As is customarily done, the real rotor is modeled as an infinite two-dimensional cascade of identical flat plate airfoils in a uniform upstream flow, as shown in Fig. 1 /20/. The flow is assumed to be two-dimensional, incompressible and inviscid. The blades do not stall, and the flow always follows the blade surface. Only the effects due to the vibration of the blades will be considered, that is, effects due to camber, thickness, and mean angle of attack will be neglected. So the assumption that the blades are flat plate aligned with the undisturbed flow is valid. The wakes are assumed to be straight and parallel to the x-axis.

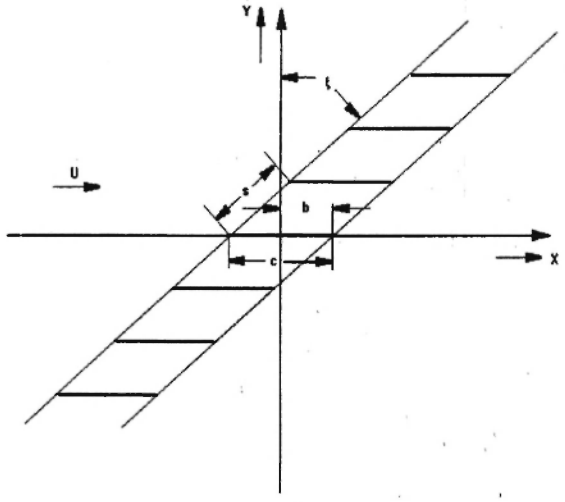

Fig. 1: Schematic of the cascade geometry

The blades are modeled as cross-sectionally rigid, equivalent section at 75% span location, as shown in Fig. 2. The blades are considered to have two degrees of freedom: heaving displacement h and torsional displacement α, about the elastic axis (EA). Displacements parallel to the chord are neglected. The effective bending stiffness and torsional rigidity of the blade are represented by springs of stiffness K_h and K_α, respectively. The blades in the cascade are assumed to execute harmonic motion with identical amplitudes and an arbitrary but constant phase angle β between adjacent blades. According to Lane's assumption[21] the phase angle β is restricted to the N_b discrete values $\beta = 2\pi n/N_b$; $n = 0,1,2,\ldots,N_b - 1$.

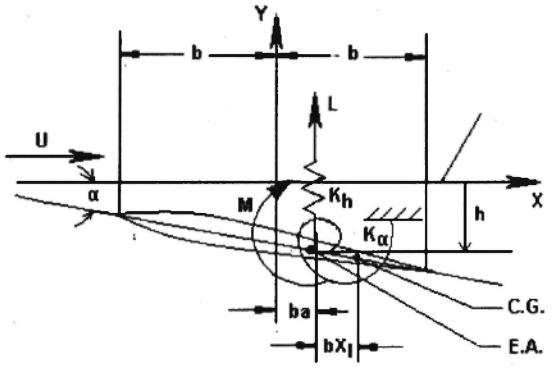

Fig. 2: Blade Geometry and Structural Model

Structural Model

The coupled bending-torsion equations of motion for the non-rotating section are:

$$m\ddot{h} + S_\alpha \ddot{\alpha} + K_h h = -LS_\alpha \ddot{h} + I_\alpha \ddot{\alpha} + K_\alpha \alpha = M \quad (1)$$

or, in matrix form

$$[M]\{\ddot{q}\} + [K]\{q\} = \{F\} \quad (2)$$

where the mass matrix [M], stiffness matrix [K], generalized coordinates {q} and force {F} are given by

$$[M] = \begin{bmatrix} m & S_\alpha \\ S_\alpha & I_\alpha \end{bmatrix}, \quad [K] = \begin{bmatrix} K_h & 0 \\ 0 & K_\alpha \end{bmatrix}$$

$$\{q\} = \begin{Bmatrix} h \\ \alpha \end{Bmatrix} \qquad \{F\} = \begin{Bmatrix} -L \\ M \end{Bmatrix}$$

Writing the aerodynamic forces in terms of nondimensionalized coefficients, and simplifying we get:

$$[S]\{\bar{q}\} = -[A]\{\bar{q}\}$$

where $[A]$ is the nondimensionalized aerodynamic coefficient matrix and $[S]$ is given by

$$[S] = \left[\bar{M}\right] - \left(1/\bar{\omega}^2\right)\left[\bar{K}\right]$$

The matrices $\left[\bar{M}\right]$ and $\left[\bar{K}\right]$ are non-dimensional mass and stiffness matrices respectively. Introducing the damping by multiplying the stiffness coefficients in bending and torsion by $(1 + ig_B)$ and $(1 + ig_t)$, respectively and simplifying we get,

$$\left(\left[\bar{M}\right]+[A]\right)\{\bar{q}\} = \frac{1}{\bar{\omega}^2}\left[\bar{K}_d\right]\{\bar{q}\} \qquad (3)$$

Multiplying both sides by $\left[\bar{K}_d\right]^{-1}$ one arrives at the eigenvalue problem in standard form /2/,

$$[D]\{\bar{q}\} = \lambda\{\bar{q}\} \qquad (4)$$

where $\lambda = 1/\bar{\omega}^2$ and the matrix $[D]$ is given by

$$[D] = \left[\bar{K}_d\right]^{-1}\left(\left[\bar{M}\right]+[A]\right)$$

$$= \frac{1}{\mu}\begin{bmatrix} \dfrac{\mu + A_{11}}{\gamma_\omega^2\left(1+ig_B\right)} & \dfrac{\mu x_I + A_{12}}{\gamma_\omega^2\left(1+ig_B\right)} \\ \dfrac{\mu x_I + A_{21}}{r_\alpha^2\left(1+ig_T\right)} & \dfrac{\mu r_\alpha^2 + A_{22}}{r_\alpha^2\left(1+ig_T\right)} \end{bmatrix}$$

Aerodynamic Model

The aerodynamic loads will be evaluated using Whitehead's theory /14/. The basic approach is to replace the blades and their wakes by the straight parallel vortex sheets and then find the distribution of vorticity along the blade which induces the correct upwash velocities normal to the blade surface along the chord of the blade. The matrix of force and moment coefficient for a cascade can be obtained using Whitehead's theory /14, 22/. The aerodynamics matrix [A] is related to the coefficient matrix [C], which is defined as (details can be found in Ref. 14 and 22)

$$C = -\frac{1}{\pi} X D^{-1} B \qquad (5)$$

where

$$C = \begin{bmatrix} C_{Fq} & C_{F\alpha} \\ C_{Mq} & C_{M\alpha} \end{bmatrix}$$

X is a 2 x n matrix whose l^{th} column ($0 \le l \le n-1$) is given by

$$\begin{bmatrix} 1 \\ \frac{1}{2}(1-\cos \pi l/n) \end{bmatrix}$$

B is a n x 2 matrix whose m^{th} row ($0 \le m \le n-1$) is given by

$$\left[1 \quad \left\{1+\frac{1}{2}i\lambda\left(1-\cos \pi\overline{2m+1}/2n\right)\right\}\right]$$

D is a n x n square matrix whose element in the l^{th} column and m^{th} row is given by

$$D_{ml} = V(-z) + i\lambda' e^{i\lambda' z}\left[-\int_z^1\left\{e^{-i\lambda' z_l}V(-z_l) + \frac{1}{2\pi z_l}\right\}dz_l\right.$$

$$\left. + \frac{I}{2}\sum_{r=0}^{\infty}\frac{\exp\{-(2\pi r+\beta)(a_c+ib_c)-i\lambda'\}}{(2\pi r+\beta)+\dfrac{i\lambda'}{a_c+ib_c}}\right]$$

$$+ i\lambda' e^{i\lambda' z}\left[\frac{1}{2\pi r}\cos \pi(2m+1)/2 \cdot \cos \pi l\right.$$

$$+\frac{1}{\pi}\sum_{r=1}^{n-1}\frac{1}{r}\cos\pi r(2m+1)/2n\cdot\cos\pi rl/n\Bigg]$$

$$+i\lambda' e^{i\lambda' z}\left[\frac{1}{2}\sum_{r=1}^{\infty}\frac{\exp\{-(2\pi r-\beta)(a_c-ib_c)-i\lambda'\}}{(2\pi r-\beta)+\dfrac{i\lambda'}{a_c-ib_c}}\right.$$

$$\left.+\frac{1}{\pi}\log_e 2\right] \qquad (6)$$

where

$$z=\frac{1}{2}\left(\cos\pi\overline{2m+1}/2n-\cos\pi l/n\right) \text{ and } \lambda' = 2k$$

and

$$V(z)=\frac{1}{4}(a+ib)\frac{\exp\{-(\pi-\beta)(a+ib)z\}}{\sinh\{\pi(a+ib)z\}}$$

$$+\frac{1}{4}(a-ib)\frac{\exp\{(\pi-\beta)(a-ib)z\}}{\sinh\{\pi(a-ib)z\}}$$

Also

$$a_c=\frac{c}{s}\cos\xi \qquad b_c=\frac{c}{s}\sin\xi$$

The elements of the nondimensional aerodynamic matrix [A] are related to the nondimensional force and moment coefficient matrix [C] as follows:

$$A_{11}=\frac{2i}{k}C_{Fq}$$

$$A_{12}=\frac{2}{k^2}\left[C_{F\alpha}-ik(1+a)C_{Fq}\right]$$

$$A_{21}=\frac{4i}{k}\left[C_{Mq}-\left(\frac{1+a}{2}\right)C_{Fq}\right] \qquad (7)$$

$$A_{22}=\frac{4}{k^2}\left[C_{M\alpha}-\left(\frac{1+a}{2}\right)C_{F\alpha}-ik(1+a)C_{Mq}+\frac{ik(1+a)^2}{2}C_{Fq}\right]$$

These relations follow directly from moving the axis from the leading edge to the elastic axis, located a distance ba behind the mid chord (Fig. 2). Taking care of differences in sign conventions between Whitehead's theory /14/ and the sign convention used in structural modeling /22/, aerodynamic matrix [A] is obtained.

Method of Solution

The integral in equation (6) is evaluated using the 16 point Gaussian quadrature. There is a singularity at $z_l = 0$ in the integral for negative values of z, which is resolved by dividing the interval into two parts, the first part from z to -ε and the second part from ε to 1.

The aeroelastic stability of the cascade is determined by the eigenvalue λ of the matrix [D]. The relation between the nondimensional frequency $\bar{\omega}$ and λ is

$$\bar{p}=\frac{i}{\sqrt{\lambda}}=\bar{p}_R+i\bar{\omega} \qquad (8)$$

where $\bar{p}$ is the nondimensionalized exponent of the time dependence $e^{\bar{p}t}$. Instability occurs when $\bar{p}_R$ becomes equal to 0.

For the given value of the number of blades, the gap-to-chord ratio, the stagger angle, the elastic axis position, and the structural parameters, the eigenvalues of the matrix [D] are calculated for a range of values of k. Denoting the values of k and $\bar{\omega}$ at which $\bar{p}_R = 0$ as k_F and $\bar{\omega}_F$, respectively, the nondimensional flutter speed can be written as

$$V_F/b\omega_T = \bar{\omega}_F/k_F$$

For getting the flutter boundary, aerodynamic loads were calculated for a given set of cascade parameters for a range of k and for all possible values of β which satisfy Lane's assumption /21/. Then the eigenvalue problem given by equation (4)

was solved and damping in torsional and bending modes was obtained. Flutter boundary is obtained for the value of β for which the damping in torsional or bending mode becomes equal to zero for minimum value of k.

Results and Discussion

Calculating the integral in the equation (6) for different values of ε it was found that the values were accurate to 10^{th} decimal place for $\varepsilon \leq 10^{-15}$. So for all calculations ε was taken as 10^{-15}. The aerodynamic coefficients calculated using the equation (5) were found to match within 4 decimal place accuracy with Whitehead's calculation /14/ as shown in Table 1.

Table 1

Comparison of the aerodynamic coefficients for present analysis and Whitehead's data /14/.

	PRESENT ANALYSIS				WHITEHEAD' ANALYSIS			
$\lambda = 0.2$	C_{Fq}		$C_{F\alpha}$		C_{Fq}		$C_{F\alpha}$	
$\beta/2\pi$								
0.0	-0.314987	-0.037316	-0.311307	-0.088716	-0.3150	-0.0373	-0.3113	-0.0887
0.1	-0.721473	0.045634	-0.729180	-0.066307	-0.7215	0.0456	-0.7292	-0.0663
0.2	-0.956517	0.032866	-0.961314	-0.110523	-0.9565	0.0329	-0.9613	-0.1105
0.3	-1.126045	0.048722	-1.133365	-0.116528	-1.1260	0.0487	-1.1334	-0.1165
0.4	-1.231017	0.078016	-1.243526	-0.100513	-1.2310	0.0780	-1.2435	-0.1005
0.5	-1.260659	0.113173	-1.279581	-0.068862	-1.2607	0.1132	-1.2796	-0.0689
0.6	-1.210008	0.149409	-1.235569	-0.025754	-1.2100	0.1494	-1.2356	-0.0258
0.7	-1.081777	0.183214	-1.113427	0.025066	-1.0818	0.1832	-1.1134	0.0251
0.8	-0.882276	0.211275	-0.918789	0.079826	-0.8823	0.2113	-0.9188	0.0798
0.9	-0.601517	0.216854	-0.639034	0.124285	-0.6015	0.2169	-0.6390	0.1243

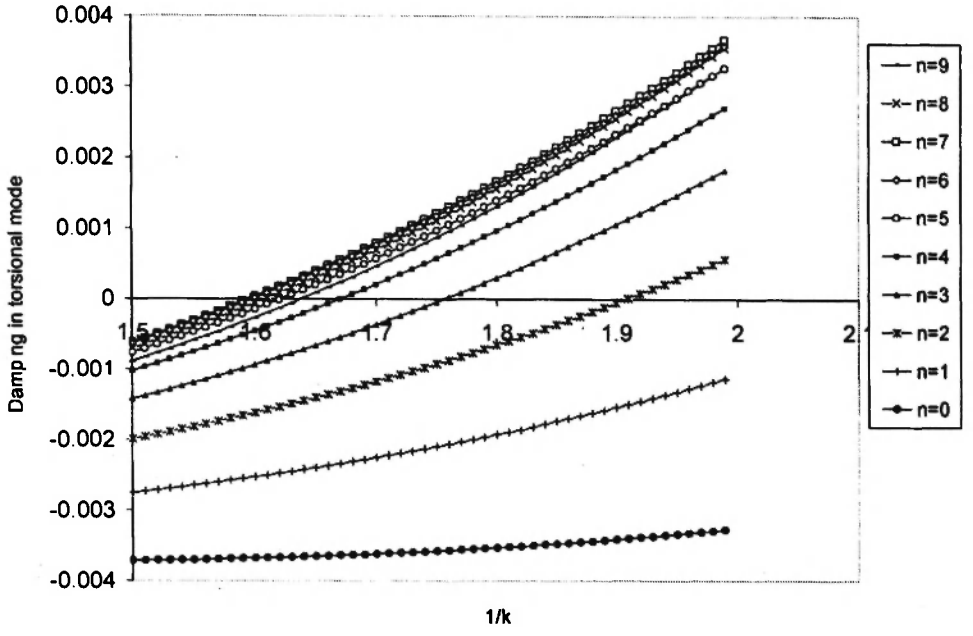

Fig. 3: Damping in torsional mode vs 1/k for different values of phase angle $\beta = 2\pi n/N_b$ ($\xi = 60^0$; s/c = 1; μ = 200; a = 0; $N_b = 40$; $r_\alpha^2 = 1/3$; $g_B = g_T = 0.005$; $x_l = 0.02$; γ_ω=0.9)

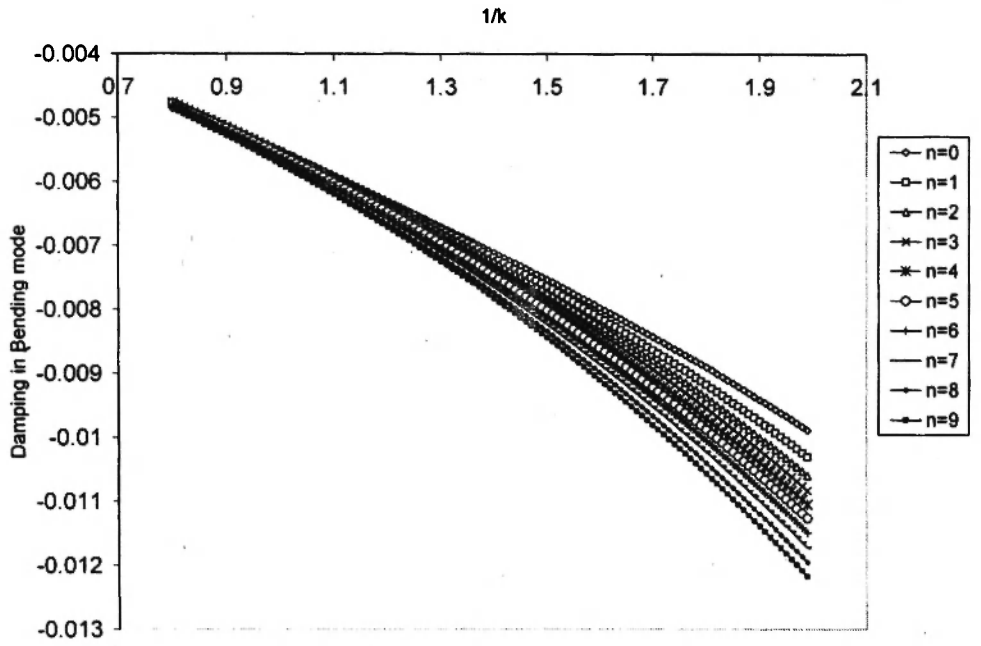

Fig. 3: Damping in bending mode vs 1/k for different values of phase angle $\beta = 2\pi n/N_b$ ($\xi = 60^0$; s/c = 1; μ = 200; a = 0; $N_b = 40$; $r_\alpha^2 = 1/3$; $g_B = g_T = 0.005$; $x_l = 0.02$; γ_ω=0.9)

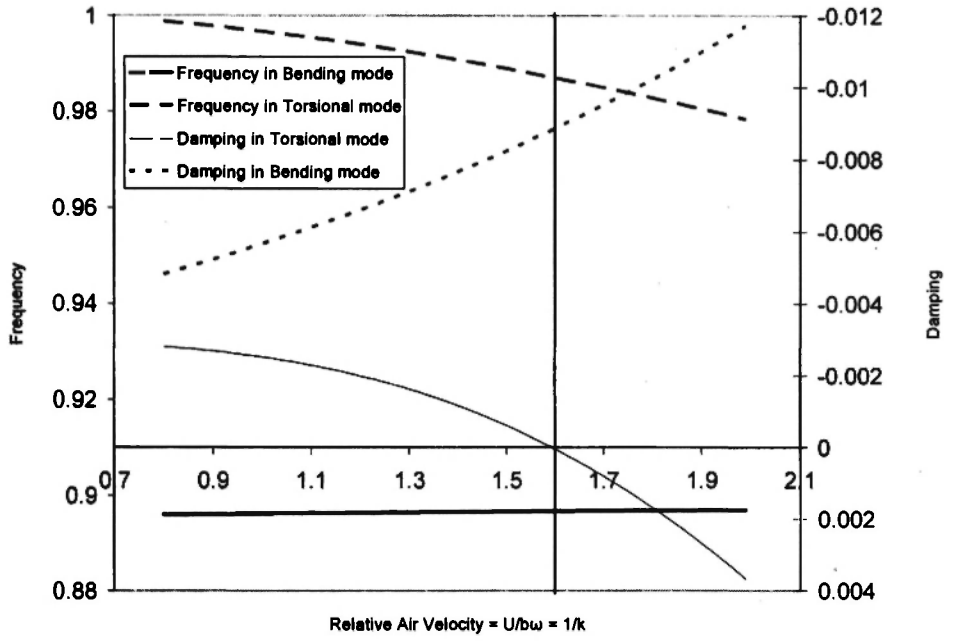

Fig. 5: Frequency and Damping in Bending and Torsion vs. 1/k ($\xi = 60^0$; s/c = 1; $\mu = 200$; a = 0; $N_b = 40$; $r_\alpha^2 = 1/3$; $g_B = g_T = 0.005$; $x_l = 0.02$; γ_ω=0.9)

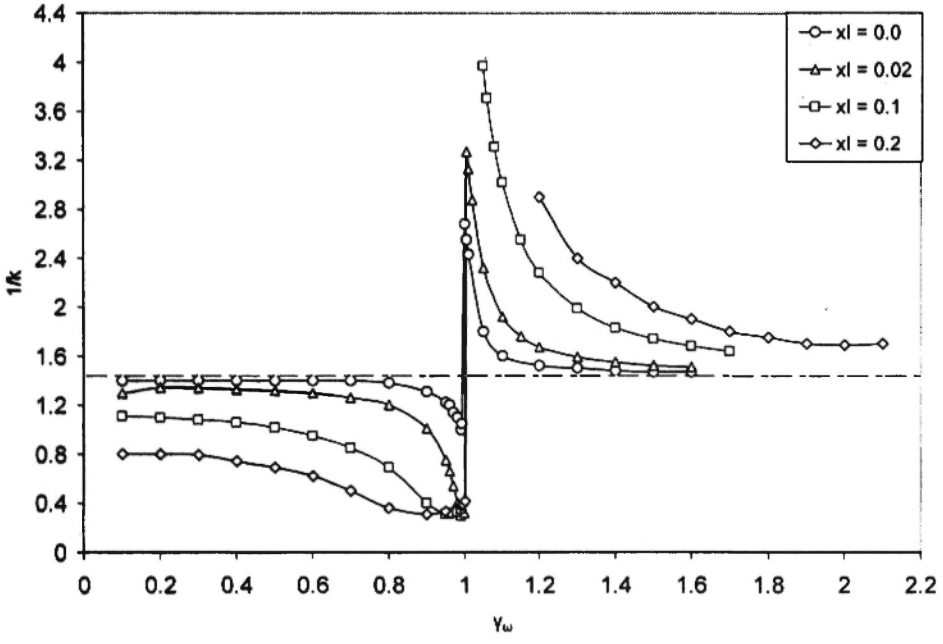

Fig. 6: Coupled Bending-Torsion flutter boundaries for EA at mid chord and no structural damping ($\xi = 60^0$; s/c = 1; $\mu = 200$; a = 0; $N_b = 40$; $r_\alpha = 1/\sqrt{3}$; $g_B = g_T = 0$)

For various values of β, the eigen value problem is solved for different values of k. The damping (real part of the eigen value) as a function of k is plotted for different β in Fig. 3. The real part of exponent for the torsional mode, representing the torsional damping, is shown in Fig. 3 as a function of reduced frequency 1/k and the interblade phase angle β (represented by n). The point where the curve crosses zero damping represents the flutter point. Flutter boundary for a particular set of structural and aerodynamic parameters is determined by minimizing it with respect to β. It can be observed from Fig. 3 that for $\xi = 60^0$; s/c = 1; μ = 200; a = 0; N_b = 40; $g_B = g_T$ = 0.005; x_I = 0.02; γ_ω=0.9, the flutter speed decreases with an increase in n (interblade phase angle), attains a minimum value at n = 7 and then starts to increase again with further increase in n. Therefore the flutter speed for the cascade being studied is minimum for n = 7, i.e. for interblade phase angle, $\beta = 2\pi n/N_b = 1.099$. Figure 4 shows the damping in bending mode for the same set of parameters. It can be observed from Fig. 4 that the cascade is not going into flutter in bending mode for the specified set of parameters.

Damping for bending and torsional mode and the frequencies of bending and torsional mode for the same set of parameters are shown in Fig. 5 for the interblade phase angle of 1.099, for which the damping for torsional mode becomes positive for minimum value of 1/k. As seen from Fig. 5, the frequency in bending mode is almost constant. The frequency in torsional mode also does not vary much. The non dimensional flutter speed is the non dimensional speed at which the damping in any of the mode becomes zero. Here in present case it is the torsional mode in which the damping reaches a value of zero at a non dimensional speed of about 1.6. The damping in bending mode keeps on becoming more and more negative, so it can be concluded that the system will be stable in the bending mode.

Figure 6 shows the effect of γ_ω, i.e. frequency ratio on the nondimensionalized flutter speed for elastic axis at mid chord and no structural damping, for a 40 bladed cascade having blade spacing to chord ratio of 1 and stagger angle of 60^0. The mass ratio, μ was taken to be 200 and nondimensional radius of gyration was taken to be $1/\sqrt{3}$. The nondimensionalized flutter speed is calculated for different values of x_I, i.e. for different values of distance between the elastic axis and C.G. Variation of x_I introduces the coupling between the bending and torsional degrees of freedom and the effect of the coupling is significant as indicated by the Fig. 6. A dip is observed in all curves around the frequency coincidence, $\gamma_\omega = \omega_B/\omega_T = 1$. It can be noted from the figure that the minimum flutter speed at the bottom of the trench is virtually independent of the coupling strength x_I, except for $x_I = 0$. With increase in x_I widening of trench can be observed. It is apparent form the figure that the coupling between the bending and torsion can be beneficial. It increases the flutter speed considerably near $\gamma_\omega = 1$. So it is important to consider the coupled problem when redesigning blades to avoid flutter problem.

Figure 7 shows the nondimensional flutter speed as function of frequency ratio for different values of x_I for a 40 bladed cascade with structural damping. It can be observed from Figures 6 and 7, by introducing a structural damping, i.e. by increasing g_B and g_T from 0 to 0.005 flutter speed increases from approximately 1.4 to 2.0. So structural damping may be used as a measure to increase the flutter speed in turbomachinery cascade. Also it can be observed that the effect of structural coupling which was introduced by increasing the distance between the elastic axis and center of mass is reduced by the introduction of structural damping. As the distance between the elastic axis and the center of mass is increased, the dip in the value of flutter speed which was observed earlier in the case of no structural damping almost disappeared.

Figure 8 shows the effect of spacing to chord ratio of the cascade on flutter speed. The flutter speed reduces from approximately 2.0 to 1.4 when the spacing to chord ratio is changed from 1 to 0.5. Also the effect of the structural coupling reduces considerably which can be observed clearly from

Figs. 7 and 8. It can be observed that the effect of centre of mass location has less influence on the flutter speed than the s/c. The difference between the value of flutter speed when the distance between the elastic axis and center of mass increases is reduced considerably with a decrease in s/c. Also the dip which was observed for s/c equal to 1 near the frequency ratio of 1 almost disappeared at s/c equal to 0.5.

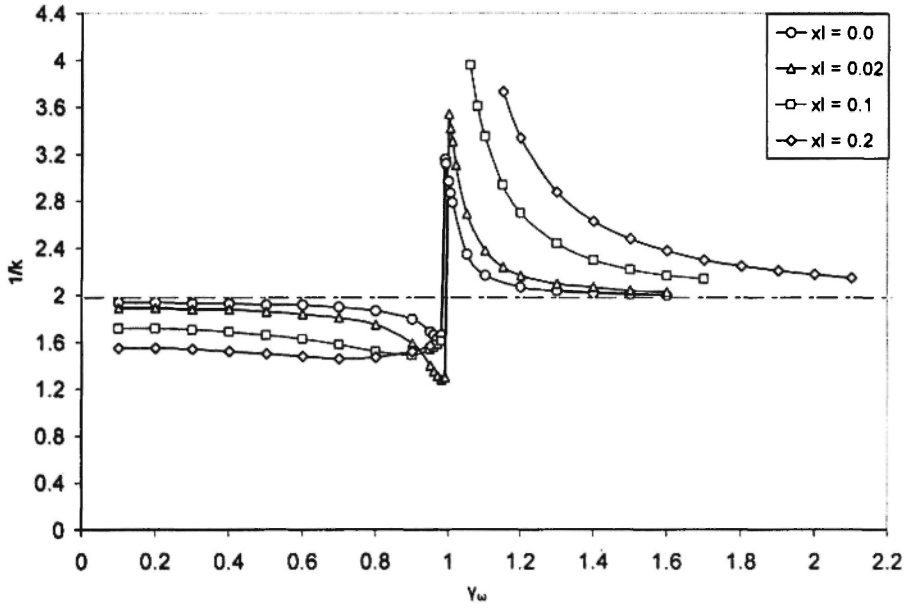

Fig. 7: Coupled Bending-Torsion flutter boundaries for EA at mid chord ($\xi = 60^0$; s/c = 1; $\mu = 200$; a = 0; N_b = 40; $r_\alpha = 1/\sqrt{3}$; $g_B = g_T = 0.005$)

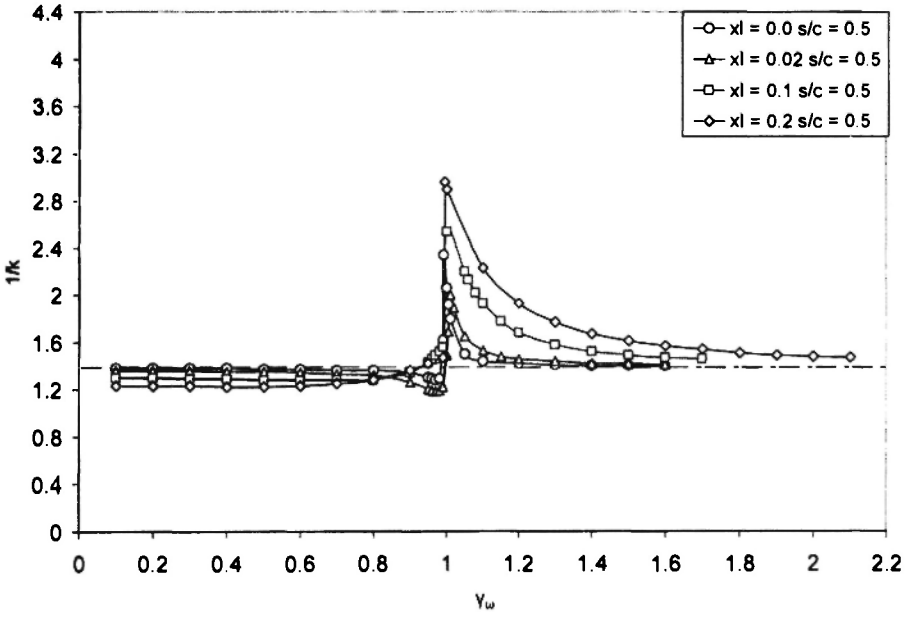

Fig. 8: Coupled Bending-Torsion flutter boundaries for EA at mid chord and s/c = 0.5 ($\xi = 60^0$; $\mu = 200$; a = 0; $N_b = 40$; $r_\alpha = 1/\sqrt{3}$; $g_B = g_T = 0.005$)

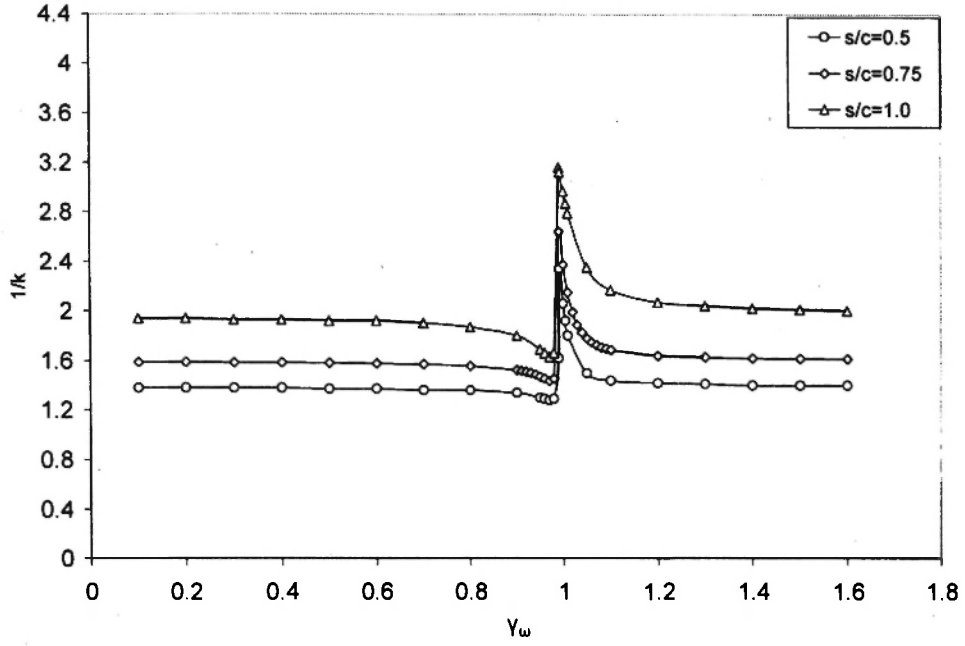

Fig. 9: Coupled Bending-Torsion flutter boundaries for EA at mid chord for different s/c ($\xi = 60^0$; $\mu = 200$; a = 0; $N_b = 40$; $r_\alpha = 1/\sqrt{3}$; $g_B = g_T = 0.005$; $x_I = 0.0$)

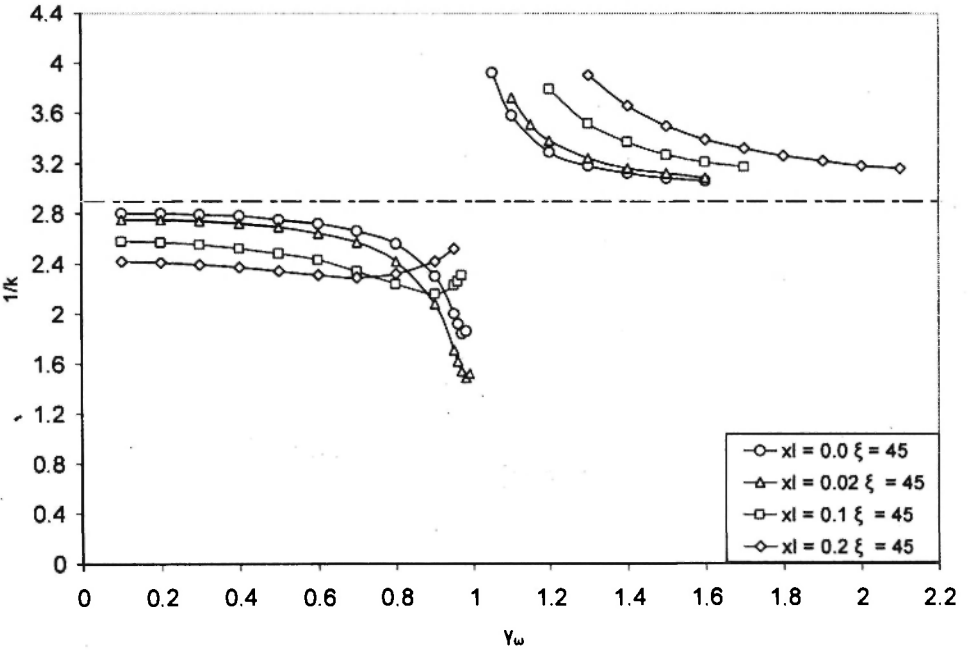

Fig. 10: Coupled Bending-Torsion flutter boundaries for EA at mid chord for stagger angle $\xi = 45^0$ ($\mu = 200$; a = 0; $N_b = 40$; $r_\alpha = 1/\sqrt{3}$; $g_B = g_T = 0.005$)

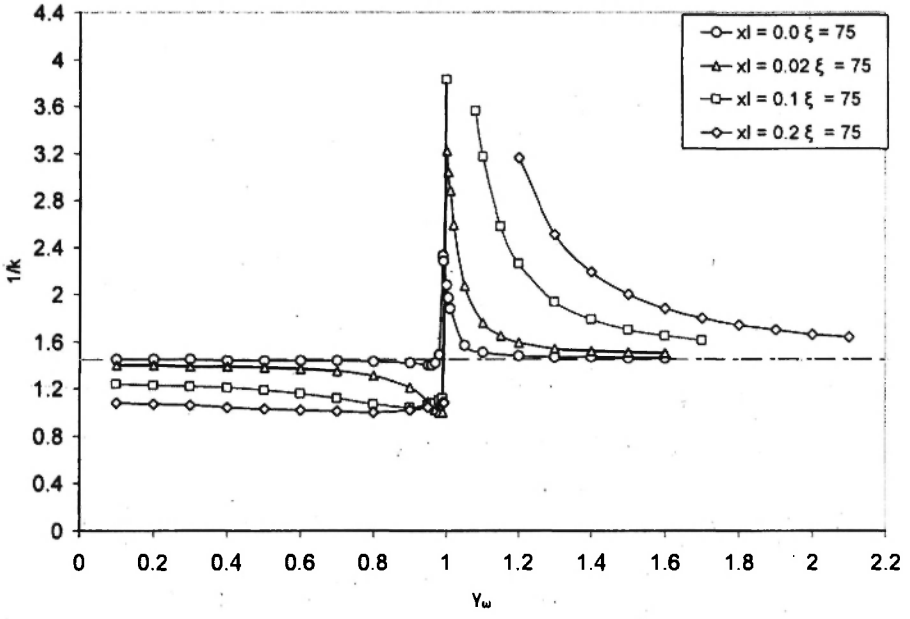

Fig. 11: Coupled Bending-Torsion flutter boundaries for EA at mid chord for stagger angle $\xi = 75^0$ ($\mu = 200$; a = 0; $N_b = 40$; $r_\alpha = 1/\sqrt{3}$; $g_B = g_T = 0.005$)

In Fig. 9 non-dimensional flutter speed as a function of frequency ratio is shown for different spacing to chord ratios for $x_l = 0.0$. It can be observed that the flutter speed keep on increasing with the increase in spacing to chord ratio and the change in the flutter speed when the frequency ratio changes also increases with the increase in spacing to chord ratio.

Figures 10 and 11 show the minimum flutter speed as a function of frequency ratio and x_l for stagger angle 45° and 75° respectively. It can be observed that with decrease in stagger angle the flutter speed increases and the effect of structural coupling also gets amplified. The dip in the value of the flutter speed near frequency ratio of 1 also increases when the stagger angle decreases. The dip is however lesser for higher values of x_l for stagger angle of 45° as compared to that for 75°.

The effect of stagger angle on flutter speed which was observed in Figs. 10 and 11 can further be seen clearly in Fig. 12 where the flutter speed is shown as a function of frequency ratio for different values of stagger angles for s/c = 1; $\mu = 200$; a = 0; $N_b = 40$; $r_\alpha^2 = 1/3$; $g_B = g_T = 0.005$; $x_l = 0.0$. It can be observed that with increase in stagger angle flutter speed decreases considerably for values of frequency ratio away from 1. However near frequency ratio of 1, the dip in the value of flutter speed is more for lower values of stagger angle as compared to higher stagger angle. So the difference between the flutter speeds for different stagger angles reduces near frequency ratio 1 as compared to that away from the frequency ratio 1.

It was observed in all the Figures that there is a jump in the flutter boundary near the frequency ratio of one. The jump can only be explained by a change in mode of vibration. Mode of vibration here is represented by the interblade phase angle. The interblade phase angle is identified in all cases and the results are shown in Figs. 13 and 14. It can be observed from these figures that the interblade phase angle changes considerable over a very narrow range around the frequency ratio equal one. This implies that as we go closer to frequency ratio of one, the system starts to switch to a different unstable mode and this mode of vibration keeps on changing over a small region.

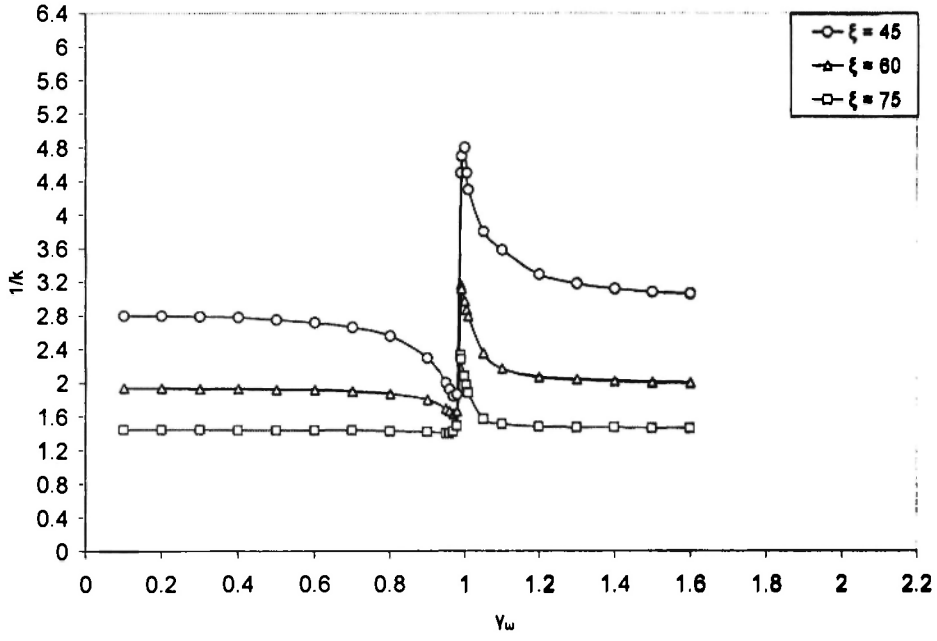

Fig. 12: Coupled Bending-Torsion flutter boundaries for EA at mid chord for different stagger angle, ξ (s/c = 1; μ = 200; a = 0; N_b = 40; $r_\alpha = 1/\sqrt{3}$; $g_B = g_T = 0.005$; $x_l = 0.0$)

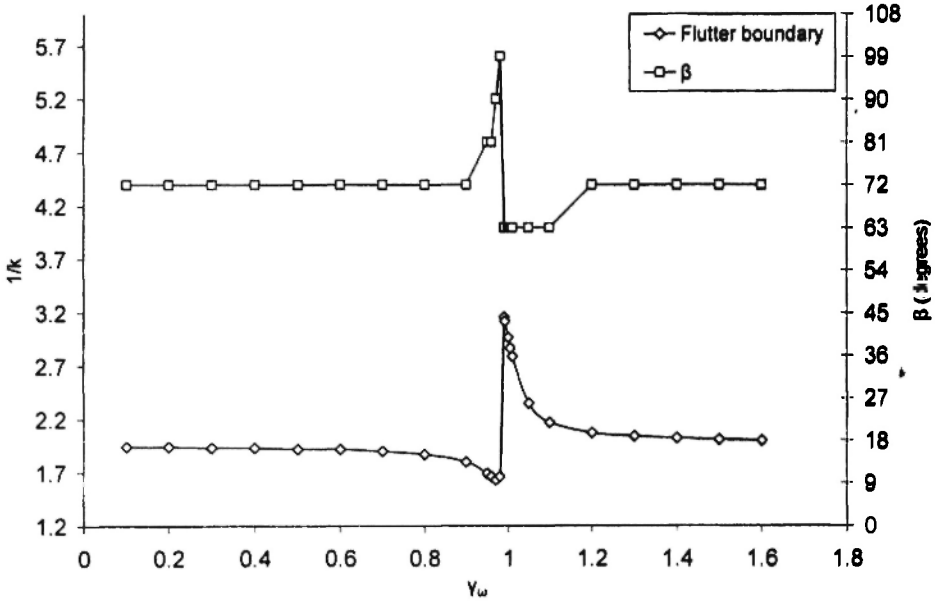

Fig. 13: Coupled Bending-Torsion flutter boundaries and interblade phase angle, β (s/c = 1; μ = 200; a = 0; N_b = 40; $r_\alpha = 1/\sqrt{3}$; $g_B = g_T = 0.005$; $x_l = 0.0$, $\xi = 60^\circ$)

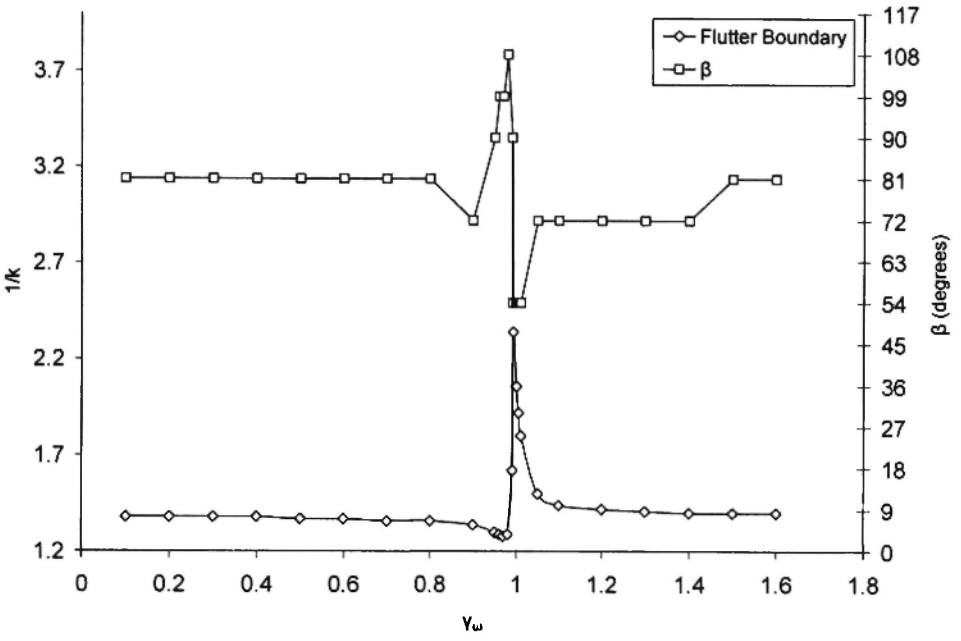

Fig. 14: Coupled Bending-Torsion flutter boundaries and interblade phase angle, β (s/c = 0.5; μ = 200; a = 0; $N_b = 40$; $r_\alpha = 1/\sqrt{3}$; $g_B = g_T = 0.005$; $x_I = 0.0$, ξ = 60°)

Conclusions

This investigation was conducted in an attempt to improve the basic understanding of the coupled bending-torsion flutter and the effect of various parameters on the flutter boundary. The aerodynamic coefficients calculated using the Whitehead's Theory, were found to match with the earlier literature results available within the limits of calculations. The effect of coupling between the bending and torsional degrees of freedom significantly changes the stability boundaries of a typical cascade. The effect of change in aerodynamic parameters of the cascade on the flutter speed was also observed. It was observed that the flutter speed in general increases with the increase in spacing to chord ratio of the cascade. Also the effect of the structural coupling increases with increase in spacing to chord ratio. With increase in stagger angle the flutter speed decreases and also the effect of structural coupling decreases. In general it was observed that the coupling between the bending and the torsional degree of freedom is beneficial and can be used for increasing the operational velocity if it is limited by the flutter. Also a cascade having higher stagger angle and lower spacing to chord ratio will have higher flutter speed. It was also concluded that the sudden jump in the flutter boundary near the frequency ratio of one is due to the change in the mode shape of vibration, i.e. the change in the interblade phase angle. It was observed that for low values of s/c, the system oscillates from one mode to other near frequency ratio one. Since there are large changes in the mode shape near frequency ratio one, this region should be avoided during the design of blade.

Acknowledgements

This work is funded by the Structures Panel of Aeronautical Research and Development Board.

References

1. Fleeter S., "Aeroelastic Research for Turbomachinery Application," American

Institute of Aeronautics and Astronautics-1977-437, 1977.

2. Srivastava R., Bakhle M. A., Keith Jr T. G., Stefko G. L., "Aeroelastic analysis of turbomachinery Part - I – phase lagged boundary condition methods," International Journal of Numerical Methods for Heat & Fluid Flow, Vol. 14, Issue 3, Apr 2004.
3. Srivastava R., Bakhle M. A., Keith Jr T. G., Stefko G. L., "Aeroelastic analysis of turbomachinery: Part II – stability computations," International Journal of Numerical Methods for Heat & Fluid Flow, Vol. 14, Issue 3, Apr 2004.
4. Reissner E., "Boundary Value Problems in Aerodynamics of Lifting Surfaces in Non-Uniform Motion," Bulletin of the American Mathematical Society, Vol. 55, No. 9, Sep. 1949.
5. Lilley G. M., "An Investigation of the Flexure-Torsion Flutter Characteristics of Airfoils in Cascade," Report No. 60, The College of Aeronautics, Cranfield, May 1952.
6. Mendelson A., Carrol R. W., "Lift and Moment Equations for Oscillating Airfoils in an Infinite Unstaggered Cascade," NACA TN-3263, Oct. 1954.
7. Chang C. C., Chu W. H., "Aerodynamic Interference of Cascade Blades in Synchronized Oscillation," Journal of Applied Mechanics, Vol 22, 1955.
8. Vogt D. M., Fransson T. H., "Effect of Blade Mode Shape on the Aeroelastic Stability of a LPT Cascade," 9th National Turbine Engine High Cycle Fatigue(HCF) conference, Pinehurst, NC, March 2004.
9. Sisto F., "Flutter of Airfoils in Cascade," Doctoral Dissertation, Massachusetts Institute of Technology, 1952.
10. Sisto F., "Unsteady Aerodynamic Reaction on Airfoils in Cascade," Journal of the Aeronautical Sciences, Vol. 22, No. 5, May 1955.
11. Lane F. and Wang C. T., "A Theoretical Investigation of the Flutter Characteristics of Compressor and Turbine Blade Systems," Wright Air Development Center Technical Report 54-449, 1954.
12. Lane F., Freidman M., "Theoretical Investigation of Subsonic Oscillatory Blade-Row Aerodynamics," NACA TN-4136, Feb. 1958.
13. Runyan H. L., Woolston D. S., Rainey A. G., "Theoretical and Experimental Investigation of the Effect of Tunnel Walls on the Forces on an Oscillating Airfoil in Two-Dimensional Subsonic Compressible Flow," NACA TN-3416, 1955.
14. Whitehead D. S., "Force and Moment Coefficients for Vibrating Aerofoils in Cascade," Great Britain A. R. C. R & M 3254, 1960.
15. Theodorsen T., "General Theory of Aero-dynamic Instability and the Mechanism of Flutter," N.A.C.A. Report 496, 1935.
16. Whitehead D.S., "Torsional Flutter of Unstalled Cascade Blades at Zero Deflection," Great Britain A. R. C. R & M 3429, 1964.
17. Whitehead D. S., "Bending Flutter of Unstalled Cascade Blades at Finite Deflection," Great Britain A. R. C. R & M 3386, 1962.
18. Bendiksen O. O., Friedmann P. P., "Coupled Bending-Torsion Flutter in Cascades with Application to Fan and Compressor Blades," UCLA-Eng-80-72, Aug 1980.
19. Kaza K. R. V., Kielb R. E., "Flutter and Response of a Mistuned Cascade in Incompressible Flow," AIAA Journal, Vol. 20, No. 8, 1982.
20. Dowell E.H., Crawley E.F., Curtiss H.C., Peters D.A., Scanlan R.H., Sisto F., A Modern Course in Aeroelasticity, Kluwer Academic Publishers, Netherlands, 2004.
21. Lane F., "System Mode Shapes in the Flutter of Compressor Blade Rows," Journal of the Aeronautical Sciences, Vol 23, No. 4, pp. 335-344, 1956.
22. Harsh Pathak, "Formulation and Solution of Coupled Bending Torsion Flutter in Turbomachinery Blades", Masters Thesis, Department of Aerospace Engineering, Indian Institute of Technology, Kanpur, 2007.